ELSEVIER

Applied Surface Science 197–198 (2002) 839–844

applied surface science

www.elsevier.com/locate/apsusc

Laser ablation thresholds of silicon for different pulse durations: theory and experiment

Harald O. Jeschke[a,*], Martin E. Garcia[a], Matthias Lenzner[b], Jörn Bonse[b], Jörg Krüger[b], Wolfgang Kautek[b]

[a]*Institute for Theoretical Physics, Freie Universität Berlin, Arnimallee 14, 14195 Berlin, Germany*
[b]*Laboratory for Thin Film Technology, Federal Institute for Materials Research and Testing, Unter den Eichen 87, 12205 Berlin, Germany*

Abstract

The ultrafast laser ablation of silicon has been investigated experimentally and theoretically. The theoretical description is based on molecular dynamics (MD) simulations combined with a microscopic electronic model. We determine the thresholds of melting and ablation for two different pulse durations $\tau = 20$ and 500 fs. Experiments have been performed using 100 Ti:Sapphire laser pulses per spot in air environment. The ablation thresholds were determined for pulses with a duration of 25 and 400 fs, respectively. Good agreement is obtained between theory and experiment.

Keywords: Laser ablation; Pulse duration; Threshold of silicon

1. Introduction

Ultrafast ablation of semiconductors induced by ultrashort laser pulses has been extensively studied in the last years, mainly because of its important technological applications [1–3]. In particular, micromachining with ultrashort laser pulses has attracted interest even in industry and medicine since the appropriate lasers have been readily available as turn-key systems. It has been demonstrated that ultrashort pulses bear the potential for precise micromachining (laterally and vertically) in a variety of materials [4]. In the course of investigations with ultrashort pulses, it became obvious that the detailed mechanisms of damage to solids caused by laser light are far from understood. Especially in the case of silicon treatment, a confusing diversity of observations, namely amorphization [5,6], melting [7], recrystallization, nucleated vaporization [8], and ablation complicates the understanding of the underlying physical phenomena. Various additional features like ripples [9,10] and columns [11,12] were observed as well.

During the last decade, many investigations have focussed on the study of the differences between the processes induced by ultrashort (fs) laser pulses and those generated by long (ns) laser pulses [13]. A general and interesting problem which has not been investigated in detail so far is the influence of the pulse duration on the ablation processes within the fs domain. In this paper, we present a combined theoretical and experimental study of the ultrafast ablation of silicon upon excitation with fs pulses of different durations.

* Corresponding author. Fax: +49-30-838-56799.
E-mail address: jeschke@physik.fu-berlin.de (H.O. Jeschke).

0169-4332/02/$ – see front matter
PII: S0169-4332(02)00458-0

2. Theory

Our approach is based upon a theory for the analysis of laser induced ultrafast processes in solids [14,15]. The theory employs molecular dynamics (MD) simulations on the basis of an electronic tight-binding Hamiltonian. This real-space calculation takes into account all atomic degrees of freedom (d.f.). Also, the strong nonequilibrium created in the electronic system by the ultrashort laser pulse is carefully treated. We calculate the nonequilibrium occupation numbers for the energy levels of the system which, being time-dependent, lead to lattice dynamics on time-dependent potential energy surfaces. This approach provides a theoretical framework for the treatment of strong nonequilibrium situations in materials where atomic and electronic d.f. play an equally important role.

In order to perform the MD simulations, a method for calculating the forces on the atoms has to be found. For this purpose, we start from the Hamiltonian

$$H = H_{\mathrm{TB}} + \sum_{i<j} \phi(r_{ij}). \tag{1}$$

The second term contains a repulsive potential $\phi(r_{ij})$ that takes care of the repulsion between the ionic cores, and the first term is a tight-binding Hamiltonian

$$H_{\mathrm{TB}} = \sum_{i\eta} \epsilon_{i\eta} n_{i\eta} + \sum_{\substack{ij\eta\vartheta \\ j\neq i}} t_{ij}^{\eta\vartheta} c_{i\eta}^{+} c_{j\vartheta}. \tag{2}$$

Here, the first term is the on-site contribution. In the second term, the $t_{ij}^{\eta\vartheta}$ are the hopping integrals, and $c_{i\eta}^{+}$ and $c_{j\vartheta}$ are creation and annihilation operators for an electron at site i or j in orbitals η or ϑ, respectively.

From the Hamiltonian of Eq. (1), we calculate the forces acting on the atoms using the Hellman–Feynman theorem

$$\boldsymbol{f}_k(\{r_{ij}(t)\}, t) = -\sum_m n(\epsilon_m, t) \langle m | \nabla_k H_{\mathrm{TB}}(\{r_{ij}(t)\}) | m \rangle - \sum_{i<j} \nabla_k \phi(r_{ij}). \tag{3}$$

Here, $|m\rangle$ stands for the eigenstate of the Hamiltonian H_{TB} that corresponds to the eigenvalue ϵ_m. The special feature of the theory which makes it applicable to optically excited materials is contained in the time-dependent occupation numbers $n(\epsilon_m, t)$ for the energy levels ϵ_m of the system. While in thermal equilibrium these occupation numbers are calculated from a Fermi–Dirac distribution function $n^0(\epsilon_m) = 2/(1 + exp\{(\epsilon_m - \mu)/k_{\mathrm{B}}T_{\mathrm{e}}\})$ at a given electronic temperature T_{e}, electronic nonequilibrium is accounted for by solving equations of motion for the occupation of electronic states [14,15]

$$\frac{\mathrm{d}n(\epsilon_m, t)}{\mathrm{d}t} = \int_{-\infty}^{\infty} \mathrm{d}\omega\, g(\omega, t - \Delta t)\{[n(\epsilon_m - \hbar\omega, t - \Delta t) + n(\epsilon_m + \hbar\omega, t - \Delta t) - 2n(\epsilon_m, t - \Delta t)]\} - \frac{n(\epsilon_m, t) - n^0(\epsilon_m)}{\tau_1}. \tag{4}$$

Thus, the electronic distribution is at each time step folded with the pulse intensity function $g(\omega, t)$. This means that at each time step, the occupation of an energy level ϵ_m changes in proportion to the occupation difference with respect to levels at $\epsilon_m - \hbar\omega$ and at $\epsilon_m + \hbar\omega$. In Eq. (4), constant optical matrix elements are assumed. The second term of Eq. (4) describes the electron–electron collisions through a rate equation of the Boltzmann type for the distribution $n(\epsilon_m, t)$. Hence, with a time constant τ_1, the distribution $n(\epsilon_m, t)$ approaches a Fermi–Dirac distribution $n^0(\epsilon_m)$.

The electron temperature T_{e} that results from the electron thermalization will not remain constant over time but will decrease due to electron–phonon coupling and to diffusion of hot electrons out of the laser excited region of the solid into colder areas. In the regime of an excitation of typically 10% of the valence electrons into the conduction band for which this theory is intended, no precise knowledge about thermal conductivity of the electrons and electron–phonon coupling constants is available. Thus, a relaxation time τ_2 which characterizes the time scale of the total decrease of the electron temperature by both the electron–phonon and by the hot electron diffusion processes is assumed

$$\frac{\mathrm{d}T_{\mathrm{e}}(t)}{\mathrm{d}t} = -\frac{T_{\mathrm{e}}(t) - T(t)}{\tau_2}. \tag{5}$$

This simple relaxation time approach has the advantage that the time scale τ_2 on which the electron–lattice equilibration takes place can be taken from experiment.

The forces of Eq. (3) can now be used to solve the equations of motion for the atoms numerically. Our study concentrates on a subregion in the center of the

irradiated area, which can change its structure, form and volume rapidly. In this way, and in contrast to the case of constant volume, part of the energy pumped into the system by the laser pulse is spent for expansion or deformation, preventing ultrafast melting [14,16]. The external pressure acting on the MD supercell is assumed to remain constant.

Therefore, we use a constant pressure MD scheme based on a Lagrangian which contains the shape and size of the MD supercell as additional d.f. [17]

$$L = \sum_{i=1}^{N} \tfrac{1}{2} m_i \dot{\boldsymbol{s}}_i^{\mathrm{T}} h^{\mathrm{T}} h \dot{\boldsymbol{s}}_i + K_{\mathrm{cell}} - \Phi(\{r_{ij}\}, t) - U_{\mathrm{cell}}. \tag{6}$$

The first term is the kinetic energy of the atoms, with the coordinates of the atoms $\boldsymbol{r}_i = h\boldsymbol{s}_i$ written in terms of the relative coordinates $\boldsymbol{s}_i$ and the 3×3-matrix h that contains the vectors spanning the MD supercell; $\dot{\boldsymbol{s}}_i$ are the relative velocity vectors, and T denotes transposition. The $\Phi(\{r_{ij}\}, t)$ is the potential which is calculated from a tight-binding formalism as explained earlier. The terms in the Lagrangian of Eq. (6) which are responsible for the simulation of constant pressure are an additional kinetic energy term K_{cell} for which the simplest form is $K_{\mathrm{cell}} = (w_{\mathrm{cell}}/2)\mathrm{Tr}(\dot{h}^{\mathrm{T}}\dot{h})$ [17], and U_{cell} is an additional potential term which describes the effect of an isotropic external pressure $U_{\mathrm{cell}} = p_{\mathrm{ext}}\Omega$; $\Omega = \det(h)$ is the volume of the MD supercell. The equations of motion are derived from Eq. (6) by the Euler–Lagrange formalism, and they are integrated numerically with the velocity form of the Verlet algorithm [18,19].

3. Experiment

Experiments were performed with a Ti:sapphire laser system which is able to produce 20 fs pulses with a maximum energy of more than 500 μJ [20]. The pulse duration can be tuned (up to 400 fs) by adding dispersive material within the inherent compressor stage. The linearly polarized pulses exhibited a center wavelength of 780 nm and a bandwidth of 50 nm. The repetition rate was kept at 1 kHz while a pulse picker selected a predefined number of shots (per spot). The pulse energy was determined by means of an OPHIR energy meter NOVA. The pulses were focused with a $R = 100$ mm spherical silver mirror onto the polished (1 1 1) surface of n-doped silicon samples in air. For the shortest pulses and higher laser fluences, the sample was placed in a slightly evacuated vacuum chamber (10^{-4} mbar). Inspection of the ablated surface regions was performed using an optical microscope in Nomarski mode. The threshold fluences were determined by plotting the squared diameter of the ablated areas in dependence on the pulse fluence and extrapolating the diameters to zero [21].

4. Results

In this section, we present theoretical and experimental results on ultrafast ablation of silicon. Simulations were performed assuming a constant external pressure of $p = 10^5$ Pa. All trajectories were calculated for an MD supercell of $N = 64$ atoms. The laser excitation of silicon was studied for different pulse durations and laser intensities. For the theoretical simulations, we considered laser pulses of Gaussian shape and duration $\tau = 20$ and 500 fs.

There are different ways to analyze the results obtained with the help of MD simulations and to determine the melting and ablation thresholds. One possibility is to analyze the changes in the bond lengths. Note that the liquid-like phase is characterized by a continuous change of lattice structure. A quantity which seems appropriate to describe this behavior is the mean square bonding length fluctuation δ

$$\delta(t) = \frac{2}{N(N-1)} \sum_{\substack{i,j \\ i>j}} \frac{\sqrt{\langle r_{ij}(t)^2 \rangle - \langle r_{ij}(t) \rangle^2}}{\langle r_{ij}(t) \rangle}. \tag{7}$$

Here $\langle\,\rangle$ defines the mean value over an MD-simulation time interval.

The dependence of $\delta(t)$ on time for different absorbed energies is shown in Fig. 1 for silicon upon excitation with laser pulses of duration $\tau = 20$ fs (see Fig. 1(a)) and $\tau = 500$ fs (see Fig. 1(b)). Absorbed energies below the damage threshold do not lead to any kind of structural change or bond-breaking process. Therefore, the corresponding δ (solid line in both curves) only shows a slight increase when the laser pulse is applied. This increase reflects the fact that

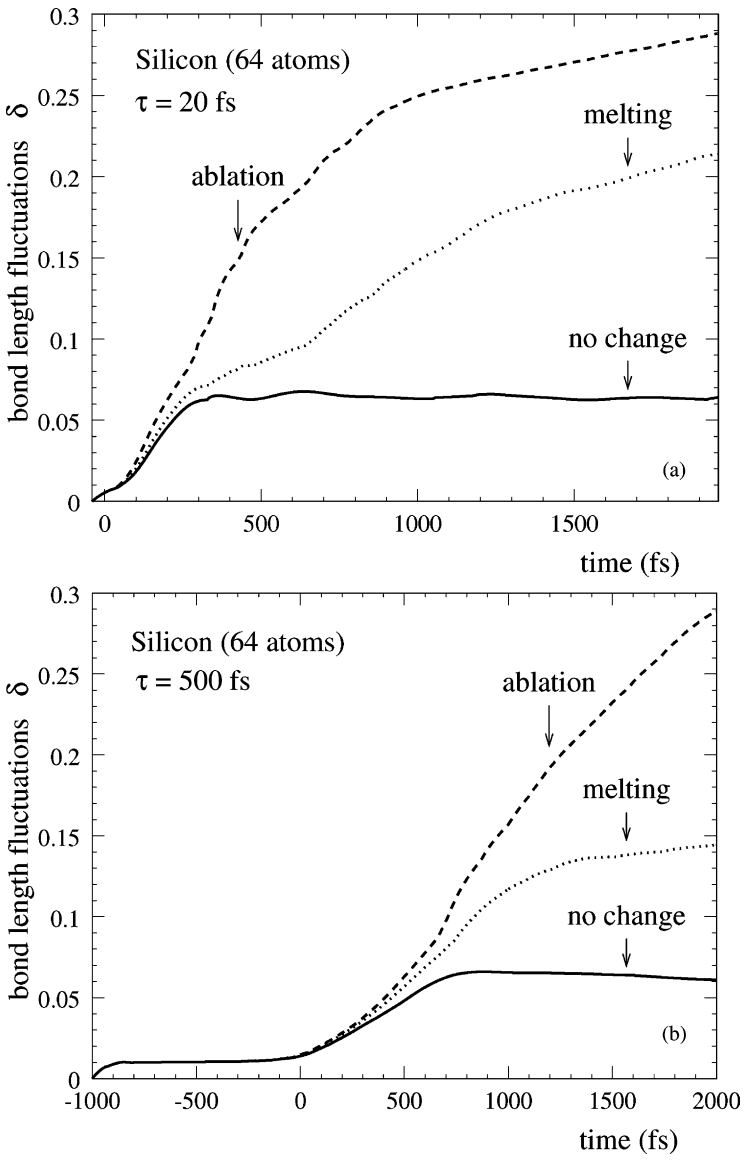

Fig. 1. Calculated time evolution of the mean square bond-length fluctuations of silicon upon excitation with a laser pulse of duration (a) 20 fs, (b) 500 fs.

electrons are excited into antibonding states, which gives rise to an effective reduction of the binding energy of the system. Consequently, it expands. The behavior of δ in this case roughly corresponds to that of the electronic temperature. Note that already 1 ps after the pulse has been switched off δ starts to decrease, reflecting the decrease of the electronic temperature due to diffusion and electron–phonon interactions.

For absorbed energies above the melting threshold, δ shows a more pronounced increase (indicated by dotted lines in both curves). For longer times, δ tends to converge to a value between 15 and 25%, depending on the absorbed energy. We have observed that a good qualitative estimate of the solid-like to liquid-like transition can be obtained assuming the validity of the Lindemann-criterion for non-equilibrium dynamics.

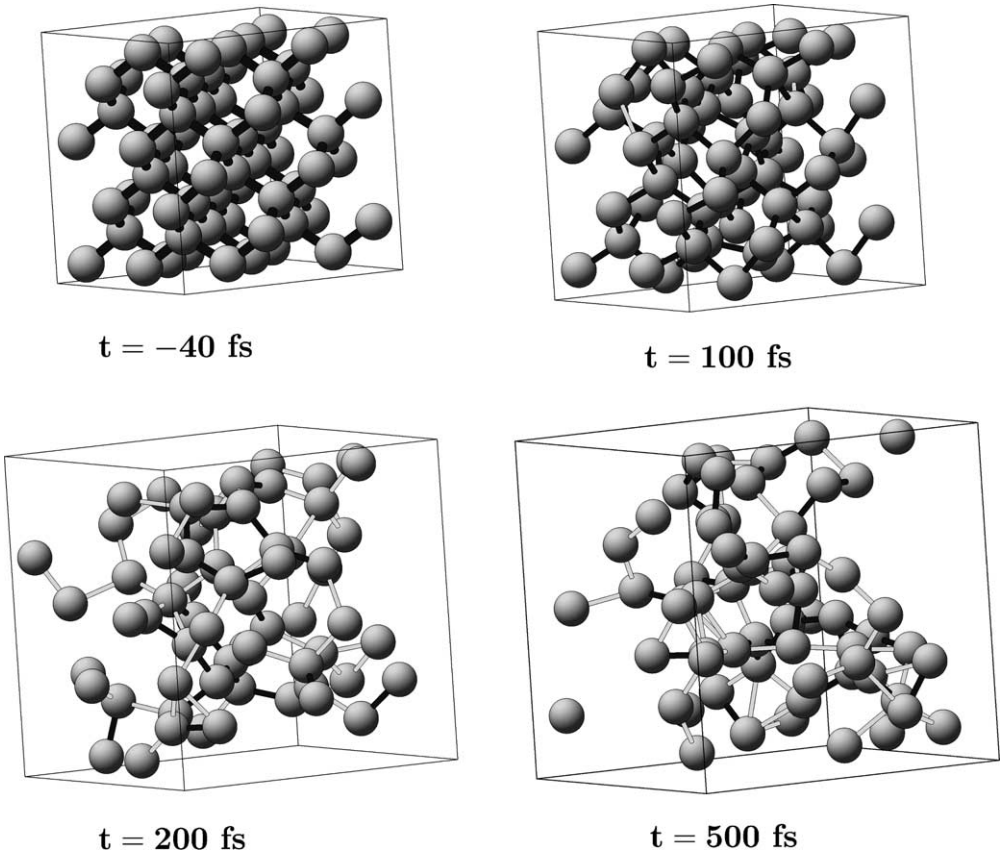

Fig. 2. Snapshots of the ultrashort ablation of silicon as a response to excitation with a laser pulse of Gaussian shape, $\tau = 20$ fs, $E_0 = 4.0$ eV per atom, $N = 64$ atoms.

This means, that the system may be considered to be molten when the bond-length-fluctuations exceed 15%.

Finally, for absorbed energies above the ablation threshold, δ exhibits a monotoneous increase in time (dashed lines), which reflects the fact that atoms (or small clusters) are removed from the system.

In order to illustrate the ablation mechanism, we show in Fig. 2, snapshots of the lattice dynamics due to excitation with a laser pulse of duration 20 fs and absorbed energy $E_0 = 4.0$ eV per atom. Note that during the first 100 fs after the peak maximum only a moderate expansion of the system occurs. Already after 200 fs, strong bond breaking processes together with a further expansion have occurred. After 500 fs, the lattice structure has suffered irreversible damage and ablation starts to take place.

In Table 1, we show the measured and calculated ablation thresholds for two different pulse durations, respectively. The trends of experimental and theoretical values regarding the dependence of the thresholds on pulse duration are in good agreement. Theoretically, the ablation threshold increases by 67% from a laser duration $\tau = 20-500$ fs, experimentally the ablation threshold increases by 65% from a laser duration $\tau = (25 \pm 5)$ to (400 ± 30) fs. The more accurate comparison is difficult since the exact values of the absorption coefficients α and β for one and two photons are required in order to convert absorbed energies per atom to fluences. Unfortunately, the values for α and β are not known for the wavelength $\lambda = 780$ nm used in theory and experiment. The time-dependent changes of the density of states induced by the laser should lead to a time dependence of the

Table 1
Ablation thresholds (theory and experiment) for different pulse durations (the theoretical values for the melting threshold are also given)

Pulse duration (fs)	Ablation threshold theory (eV per atom)	Ablation threshold experiment (J/cm^2)	Melting threshold theory (eV per atom)
20	3.7 ± 0.3		2.6 ± 0.3
25 ± 5		0.17 ± 0.015	
400 ± 30		0.28 ± 0.030	
500	6.2 ± 0.5		5.4 ± 0.4

absorption coefficients α and β [22]. A more detailed analysis of this problem is required [23].

5. Summary

The ablation thresholds of silicon upon excitation with fs laser pulses of different durations were studied experimentally and theoretically. Good agreement between theory and experiment in the dependence of the ablation threshold on pulse duration is obtained.

References

[1] J.S. Horwitz, H.-U. Krebs, K. Murakami, M. Stuke (Eds.), Proceedings of the Fifth International Conference on the Laser Ablation, Goettingen, 1999, Appl. Phys. A Mater. Sci. Process. 69 (1999) S1–S952.
[2] J. Krüger, W. Kautek, Laser Phys. 9 (1999) 30.
[3] K. Sokolowski-Tinten, J. Bialkowski, D. von der Linde, Phys. Rev. B 51 (1995) 14186, and references therein.
[4] D. Bäuerle, Laser Processing and Chemistry, 3rd Edition, Springer, Heidelberg, Berlin, 2000.
[5] P.L. Liu, R. Yen, N. Bloembergen, R.T. Hodgson, Appl. Phys. Lett. 34 (1979) 864.
[6] S. Higashi, T. Sameshima, Jpn. J. Appl. Phys. 40 (2001) 480.
[7] C.V. Shank, R. Yen, C. Hirlimann, Phys. Rev. Lett. 50 (1983) 454.
[8] A. Cavalleri, K. Sokolowski-Tinten, J. Bialkowski, M. Schreiner, D. van der Linde, J. Appl. Phys. 85 (1999) 3301.
[9] P.M. Fauchet, A.E. Siegman, Appl. Phys. Lett. 40 (1982) 824.
[10] G.K. Giust, T.W. Sigmona, Appl. Phys. Lett. 70 (1997) 3552.
[11] T.H. Her, R.J. Finlay, C. Wu, S. Deliwala, E. Mazur, Appl. Phys. Lett. 73 (1998) 1673.
[12] A.J. Pedraza, J.D. Fowlkes, D.H. Lowndes, Appl. Phys. Lett. 77 (2000) 3018.
[13] R.F.W. Herrmann, J. Gerlach, E.E.B. Campbell, Appl. Phys. A 66 (1998) 35.
[14] H.O. Jeschke, M.E. Garcia, K.H. Bennemann, Phys. Rev. B 60 (1999) R3701.
[15] H.O. Jeschke, M.E. Garcia, K.H. Bennemann, Phys. Rev. Lett. 87 (2001) 015003.
[16] H.O. Jeschke, M.E. Garcia, K.H. Bennemann, Appl. Phys. A 69 (1999) 49.
[17] M. Parrinello, A. Rahman, J. Appl. Phys 52 (1981) 7182.
[18] L. Verlet, Phys. Rev. 159 (1967) 98.
[19] J.M. Haile, Molecular Dynamics Simulation: Elementary Methods, Wiley, New York, 1975.
[20] M. Lenzner, Ch. Spielmann, E. Wintner, F. Krausz, A.J. Schmidt, Opt. Lett. 20 (1995) 1397.
[21] J.M. Liu, Opt. Lett. 7 (1982) 196.
[22] H.O. Jeschke, M.E. Garcia, K.H. Bennemann, cond-mat/0107230.
[23] Work in this direction is in progress.